

University of Groningen

## Propagating the Kadanoff-Baym equations for atoms

Dahlen, Nils Erik; Stan, Adrian

*Published in:*  
Journal of Physics, Conference Series

**IMPORTANT NOTE: You are advised to consult the publisher's version (publisher's PDF) if you wish to cite from it. Please check the document version below.**

*Document Version*  
Publisher's PDF, also known as Version of record

*Publication date:*  
2006

[Link to publication in University of Groningen/UMCG research database](#)

*Citation for published version (APA):*  
Dahlen, N. E., & Stan, A. (2006). Propagating the Kadanoff-Baym equations for atoms. *Journal of Physics, Conference Series*, 35(2).

### Copyright

Other than for strictly personal use, it is not permitted to download or to forward/distribute the text or part of it without the consent of the author(s) and/or copyright holder(s), unless the work is under an open content license (like Creative Commons).

### Take-down policy

If you believe that this document breaches copyright please contact us providing details, and we will remove access to the work immediately and investigate your claim.

*Downloaded from the University of Groningen/UMCG research database (Pure): <http://www.rug.nl/research/portal>. For technical reasons the number of authors shown on this cover page is limited to 10 maximum.*

# Propagating the Kadanoff-Baym equations for atoms and molecules

Nils Erik Dahlen, Robert van Leeuwen and Adrian Stan

Theoretical Chemistry, Materials Science Centre, Rijksuniversiteit Groningen, Nijenborgh 4, 9747 AG Groningen, The Netherlands

E-mail: n.e.dahlen@rug.nl

**Abstract.** While the use of Green's function techniques has a long tradition in quantum chemistry, the possibility of propagating the Kadanoff-Baym equations has remained largely unexplored. We have implemented the time-propagation for atoms and diatomic molecules, starting from a system in the groundstate. The initial stage of the calculation requires solving the Dyson equation self-consistently for the equilibrium Green's function. This Green's function contains a huge amount of information, and we have found it particularly interesting to compare the self-consistent total energies to the results of variational energy functionals of the Green's function. We also use time-propagation for calculating linear response functions, as a means for obtaining the excitation energies of the system. We have presently implemented the propagation for the second Born approximation, while the *GW* approximation has now been implemented for the ground state calculations.

## 1. Introduction

The use of Green's functions has a long history in quantum chemistry as a method for calculating total energies, ionization potentials, and excitation energies, and a number of other properties [1, 2]. The concept of conserving approximations [3, 4] has, however, not been given much attention, and the Keldysh formalism [5, 6] for treating non-equilibrium systems has remained largely unexplored. The interest in using non-equilibrium Green's function techniques has lately been stimulated by the arrival of molecular electronics, and the need for first-principles calculations on non-equilibrium systems. Green's function techniques are in this context highly interesting as a complementary method to time-dependent density functional theory (TDDFT) [7], which is the method of choice for a realistic treatment of large systems. TDDFT employs an auxiliary system of non-interacting electrons moving in an effective potential  $v_s[n](\mathbf{r}, t)$ . This potential is a functional of the time-dependent density. The existing functionals are, however, not sufficient for a good description even of steady-state transport. The most important flaw is that the commonly used functionals are *local* functionals of the density, in the sense that  $v_s[n](\mathbf{r}, t) = v_s[n(\mathbf{r}, t)]$ . Improved functionals should take into account also the history of the system. Non-equilibrium Green's function techniques are in this respect useful for two main reasons: Firstly, solving the Kadanoff-Baym equations we can provide benchmark results for testing new TDDFT functionals. Secondly, diagrammatic techniques can be used to systematically derive improved density functionals [8].

In this paper, we study atoms and small diatomic molecules in the ground state and in an applied electric field. The systems are initially in the ground state, which means that the

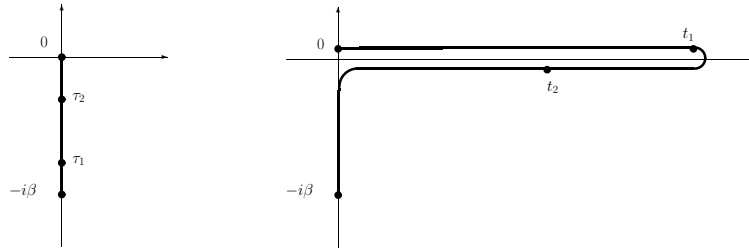


**Figure 1.** At  $t = 0$ , the system is in thermal equilibrium. The first step is therefore to calculate the Green's function for imaginary times from 0 to  $-i\beta$ . Describing the system for times  $t > 0$  implies calculating  $G_{ij}(t_1, t_2)$  on an extending time-contour.

initial correlations are conveniently accounted for by extending the time-contour, as illustrated in Fig. 1, with an imaginary branch going from  $t = 0$  to  $-i\beta$ , where  $\beta = 1/k_B T$ . As we are here concerned with very small systems, we are obviously only interested in the limit  $T \rightarrow 0$ . The calculations thus consists of two steps: 1) First, we solve the Dyson equation to self-consistency for the equilibrium system. This implies calculating the Green's function for time-arguments on the imaginary axis from  $t = 0$  to  $t = -i\beta$ . At this stage, the Green's function only depends on the difference between its imaginary time-coordinates. 2) We then propagate the Green's function in order to find the Green's function for one or two coordinates on the real time-axis. The contribution from the functions with one argument on the imaginary axis accounts for the initial correlations.

## 2. Reference state and basis functions

The calculations are carried out using a set of basis function, such that

$$G(\mathbf{x}t, \mathbf{x}'t') = \sum_{ij} \phi_i(\mathbf{x}) G_{ij}(t, t') \phi_j^*(\mathbf{x}'), \quad (1)$$

where the space- and spin variables are denoted by  $\mathbf{x} = (\mathbf{r}, \sigma)$ . Introducing a finite basis reduces the Kadanoff-Baym equations to a set of coupled matrix equations. The basis functions  $\phi_i(\mathbf{x})$  are chosen to be molecular orbitals obtained from either Hartree-Fock or DFT calculations. These molecular orbitals are themselves represented as linear combinations of Slater functions,  $\phi_i(\mathbf{x}) = \sum_j \psi_j(\mathbf{x}) U_{ji}^\dagger$ , where the Slater functions  $\psi_i(\mathbf{x}) = \chi_i(\sigma) r^{n_i-1} e^{-\lambda_i r} Y_{l_i}^{m_i}(\Omega)$  are centered on the nuclei of the molecule. The observables calculated from the Green's function will not depend on whether the molecular orbitals are obtained from HF or DFT calculations, but they will depend essentially on the Slater basis  $\psi_j(\mathbf{x})$ . The Slater basis should not only be sufficient for representing the electron charge, but should also approximate a complete basis set in the region where the charge is located. They should in this sense also account for the continuum states, and the set of molecular orbitals  $\phi_j(\mathbf{x})$  will for this reason include orbitals with rather high orbital energies. We have chosen the basis by checking convergence of the ground state value for the total energy and ionization potentials.

The molecular orbitals by construction diagonalize the matrix  $[h + \Sigma_0]_{ij} = \delta_{ij} \epsilon_i$ , where the noninteracting Hamiltonian matrix

$$h_{ij} = \int d\mathbf{x} \phi_i^*(\mathbf{x}) [-\nabla^2/2 + w(\mathbf{r})] \phi_j(\mathbf{x}) - \delta_{ij} \mu \quad (2)$$

contains the potential due to the nuclei  $w(\mathbf{r})$ , and the chemical potential  $\mu$ . The self-energy  $\Sigma_0$  can be either the HF potential,  $v_H + \Sigma_x$ , or  $v_H + v_{xc}$  if the orbitals are obtained from a DFT

calculation. Due to the inclusion of the chemical potential in the definition of  $h$ , negative values of the orbital eigenvalues  $\epsilon_i$  correspond to occupied states, and positive values to unoccupied states. We stress that the value of the chemical potential can be chosen arbitrarily. As long as it is located in the gap between the highest occupied and the lowest unoccupied level, the observables calculated from the Green's function will not depend its value.

The orbital eigenvalues can also be used to define an equilibrium Green's function for the HF or DFT system. Defined for complex time-arguments,  $-i\tau$ , where  $-\beta \leq \tau \leq \beta$ , the Matsubara Green's function takes the well-known form

$$G_{0,ij}(\tau) = \delta_{ij}\theta(\tau)[f(\epsilon_i) - 1]e^{-\tau\epsilon_i} + \delta_{ij}\theta(-\tau)f(\epsilon_i)e^{-\tau\epsilon_i}, \quad (3)$$

where  $f(\epsilon)$  is the Fermi distribution. This Green's function is diagonal in the molecular orbital basis, and solves the Dyson equation

$$[-\partial_\tau - h - \Sigma_0]G_0(i\tau) = \delta(\tau). \quad (4)$$

Importantly,  $G_0$  is anti-periodic,  $G_0(\tau) = -G_0(\tau - \beta)$ , and is for this reason highly useful as a reference Green's function when finding the interacting ground state Green's function, as discussed below. In Eq. (4), as well as in the remainder of this paper, all the quantities are now time-dependent matrices, where the indices refer to the molecular orbital basis.

### 3. Initial state

The first stage of the calculation involves finding the ground state Green's function, which has both time-arguments on the imaginary branch of the contour and only depends on the difference between the time-coordinates. Defining  $G^M(\tau - \tau') = -iG(-i\tau, -i\tau')$ , and  $\Sigma^M(\tau - \tau') = -i\Sigma(-i\tau, -i\tau')$ , we can solve the Dyson equation  $[-\partial_\tau - h]G^M(\tau) = \delta(\tau) + \int d\bar{\tau} \Sigma^M(\tau - \bar{\tau})G^M(\bar{\tau})$ . By using the reference Green's function  $G_0$ , we can write the Dyson equation on the integral form,

$$G^M(\tau) = G_0(\tau) + \int_0^\beta d\tau' \int_0^\beta d\tau'' \tilde{G}_0(\tau - i\tau')\tilde{\Sigma}(\tau' - \tau'')G^M(\tau''), \quad (5)$$

where  $\tilde{\Sigma}[G^M](\tau) = \Sigma^M[G^M](\tau) - \delta(\tau)\Sigma_0$ . Employing  $G_0$  has the advantage that the resulting  $G^M$  will now automatically also be anti-periodic,  $G^M(\tau - \beta) = -G^M(\tau)$ . The self-energy is a functional of the Green's function, and the Dyson equation should for this reason be solved to self-consistency. The equation is solved by an iterative algorithm analogous to the biconjugate gradient method from linear algebra. It is important to note that the physical observables calculated from the Green's function will be independent of the choice of a reference Green's function, as long as  $G_0$  satisfies the correct boundary conditions.

It is inconvenient to represent the Green's function and the self-energy on an even-spaced time-grid, as they are both strongly peaked around the points  $\tau = 0$  and  $\tau = \pm\beta$ . This is easily seen from the definition of the non-interacting Green's function in Eq. (3), which contains the exponential terms  $e^{-\epsilon_i\tau}$ . If the system has large negative eigenvalues, we need a rather fine time-mesh to account for the terms rapidly decaying away from these endpoints. For this reason, we calculate  $G^M(\tau)$  on a uniform power mesh, which is dense around the endpoints 0 and  $\pm\beta$  [9, 10]. As we are interested in the  $T \rightarrow 0$  limit, the parameter  $\beta$  must be large enough so that changing it with a small amount does not influence the results.

We have carried out the ground-state calculations within two different self-energy approximations; the second-order approximation and the  $GW$  approximation. For a given  $G^M$  matrix, the second-order self-energy matrix (for a spin-unpolarized system) is

$$\Sigma_{ij}^M(\tau) = - \sum_{klmnpq} G_{kl}^M(\tau)G_{mn}^M G_{pq}^M(-\tau)v_{iqmk}(2v_{lnpj} - v_{nlpj}), \quad (6)$$

$$\begin{aligned}
\text{a)} \quad \Sigma_c^{(2)} &= \text{[Diagram 1]} + \text{[Diagram 2]} \\
\text{b)} \quad \Sigma_c^{\text{GW}} &= \text{[Diagram 1]} + \text{[Diagram 3]} + \dots
\end{aligned}$$

**Figure 2.** We have considered two conservative approximations: The second Born approximation illustrated in (a), and the  $GW$  approximation illustrated in (b).

where the two-electron integrals are defined according to

$$v_{ijkl} = \int \int d\mathbf{x} d\mathbf{x}' \phi_i^*(\mathbf{x}) \phi_j^*(\mathbf{x}') v(\mathbf{r} - \mathbf{r}') \phi_k(\mathbf{x}') \phi_l(\mathbf{x}). \quad (7)$$

Both these self-energy functionals are examples of conserving approximations [3, 4], which can be derived from an underlying functional  $\Phi$ , according to  $\Sigma[G] = \delta\Phi/\delta G$ . The correlation part of the self-energy diagrams are shown in Fig. 2. The use of conserving approximations is essential not only for time-propagation, where e.g. the momentum and total energy should evolve in agreement with macroscopic conservation laws. For ground state calculations, they give physically consistent and unambiguous values for the resulting observables [10].

The ground state Green's function provides a wealth of information about the system. The total energy is calculated from

$$E = \text{Tr} \{hG^M(0^-)\} + \frac{1}{2} \int_0^\beta d\tau \text{Tr} \{\Sigma^M(-\tau)G^M(\tau)\} + \mu N. \quad (8)$$

There are many other ways to calculate the total energy from the Green's function, but only when it is a self-consistent solution obtained from a conserving self-energy approximation do they all yield the same result. We have found it highly interesting to compare our self-consistent total energies to those obtained from the Luttinger-Ward (LW) functional [11] evaluated on an approximate non-interacting Green's function. This energy functional is variational in the sense that  $\delta E_{\text{LW}}[G]/\delta G = 0$  when  $G$  is a self-consistent solution. Evaluating the functional at an approximate Green's function  $\tilde{G}$  will then give an error only to second order in  $\Delta G = \tilde{G} - G$ . Due to the stability of the LW functional, it produces a value very close to the self-consistent result when evaluated on, e.g. a Hartree-Fock Green's function [10, 12].

There are several possibilities for calculating ionization potentials from the ground state Green's function. One obvious method would be to Fourier transform  $G^M(\tau)$ , producing  $G^M(\omega_n)$  on the Matsubara frequencies  $\omega_n = i(2n + 1)\pi/\beta$ . The Green's function on the real frequency axis can then be obtained by a Pade approximation, and the ionization potentials are then found as the poles of this quantity [9]. This procedure is rather cumbersome, and we have preferred to calculate the ionization potentials from the Extended Koopmans' Theorem [13]. The method is based on defining the  $N - 1$ -particle states  $|\xi_i^{N-1}\rangle = \int d\mathbf{x} u_i^*(\mathbf{x}) \hat{\psi}(\mathbf{x}) |\Psi_0^N\rangle$ , and then optimizing the coefficients  $u_i(\mathbf{x})$  according to  $\delta \left[ \langle \xi_i^{N-1} | \hat{H} | \xi_m^{N-1} \rangle - \lambda_i \langle \xi_i^{N-1} | \xi_i^{N-1} \rangle \right] / \delta u_i^*(\mathbf{x}) = 0$ . This results in the eigenvalue equation

$$\Delta u = u \rho \tilde{\lambda}, \quad (9)$$

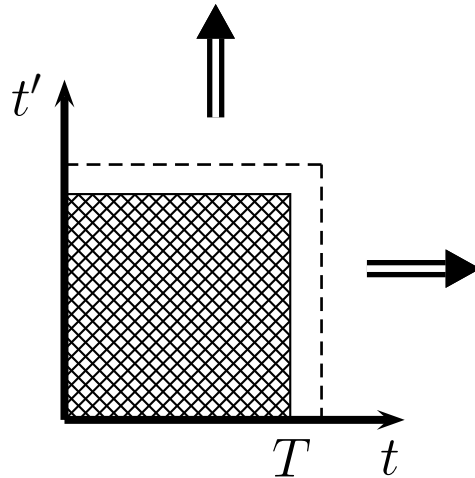


**Figure 3.** The Green's function  $G^{\lessgtr}(t, t')$  is represented for time-arguments within an expanding square defined by  $t, t' \leq T$ .

where the density matrix  $\rho_{ij} = G_{ij}^M(0^-)$  and  $\Delta_{ij} = -\partial_\tau G_{ij}^M(\tau)|_{\tau=0^-}$  are both given by the equilibrium Green's function, and the eigenvalues are  $\tilde{\lambda}_i = E_m^{N-1} - E_0^N + \mu$ . It can be shown [14] that the EKT is exact for the first ionization potential  $I_p = \lambda_1 - \mu$ . If the Green's function used in this scheme is the Hartree-Fock Green's function, the eigenvalue problem (9) reduces to the Hartree-Fock equations.

#### 4. Propagation

Once the ground state Green's function has been calculated, it can be propagated according to the Kadanoff-Baym equations [6]. Time-propagation means that the contour which initially goes along the imaginary axis from  $t = 0$  to  $t = -i\beta$  is extended along the real axis, as illustrated in Fig. 1. The Green's function with both arguments on the real time-axis are represented by the functions  $G^{\lessgtr}(t, t')$ , related by the symmetry  $[G_{ij}^{\lessgtr}(t, t')]^* = -G_{ji}^{\lessgtr}(t', t)$  and the boundary condition  $G_{ij}^>(t, t) - G_{ij}^<(t, t) = -i\delta_{ij}$ . We also need to calculate the functions  $G^{\lrcorner}(t, i\tau)$  and  $G_{ij}^{\lrcorner}(i\tau, t)$  with one real and one imaginary time-argument. The implementation of the propagation is similar to the scheme described by Köhler *et. al.* in Ref. [15].

Compared to the propagation scheme described in Ref. [15], there are two main differences. Firstly, these equations are propagated for an inhomogeneous system, i.e. the Green's functions and  $h_{\text{HF}}$  are time-dependent matrices rather than vectors. This significantly increases the size of the objects to be calculated. Furthermore, the complicated structure of the Green's function matrix can make time-propagation unstable. This is particularly true if the basis includes orbitals with very large eigen energies. The matrix elements then oscillate with on a time-scale given by the eigenvalue differences  $\epsilon_i - \epsilon_j$ . While the equilibrium Green's function matrix  $G_{ij}^M(\tau)$  is dominated by the diagonal terms, the rapidly oscillating off-diagonal terms play an important role during the time-propagation. The effects are not that apparent when considering time-dependent observables such as the dipole-moment. The total energy is on the other hand much more sensitive to the size of the time-steps. One should also keep in mind that the systems considered here only have discrete energy levels. The continuous part of the energy spectrum is represented by a set of orbitals which can have rather large eigenvalues, but they will not cause damping effects similar to what is observed in systems with a continuous spectrum [16].

The other main difference is found in the initial correlations, which in our case is specified by the equilibrium Green's function. At the start of the propagation, the initial conditions are given by  $G^<(0,0) = iG^M(0^-)$ ,  $G^>(0,0) = iG^M(0^+)$ ,  $G^{\lceil}(t, i\tau) = iG^M(-\tau)$ , and  $G^{\lceil}(i\tau, t) = iG^M(\tau)$ . Due to the anti-periodicity of  $G^M(\tau)$ , the resulting non-equilibrium Green's function will automatically satisfy the Kubo-Martin-Schwinger boundary condition  $G(t_i, t) = -G(t_f, t)$ , where  $t_i$  is the initial point of the Keldysh contour (at  $t = 0$ ) and  $t_f$  is the end-point at  $t = -i\beta$ .

By using the symmetry of the Green's functions, we only calculate  $G^>(t, t')$  for  $t > t'$  and  $G^<(t, t')$  for  $t \leq t'$ . This means that we have to solve the Kadanoff-Baym equations on the form

$$i\partial_t G^>(t, t') = h(t)G^>(t, t') + I_1^>(t, t') \quad -i\partial_{t'} G^<(t, t') = G^<(t, t')h(t') + I_2^<(t, t') \quad (10)$$

and

$$i\partial_t G^{\lceil}(t, \tau) = h(t)G^{\lceil}(t, \tau) + I^{\lceil}(t, \tau). \quad -i\partial_t G^{\lceil}(\tau, t) = G^{\lceil}(\tau, t)h(t) + I^{\lceil}(\tau, t). \quad (11)$$

The collision integrals are

$$\begin{aligned} I_1^>(t, t') &= \int_0^t d\bar{t} [\Sigma^R(t, \bar{t})G^>(\bar{t}, t') + \Sigma^>(t, \bar{t})G^A(\bar{t}, t')] + \frac{1}{i} \int_0^\beta d\bar{\tau} \Sigma^{\lceil}(t, -i\bar{\tau})G^{\lceil}(-i\bar{\tau}, t') \quad (12) \\ I_2^<(t, t') &= \int_0^{t'} d\bar{t} [G^R(t, \bar{t})\Sigma^<(\bar{t}, t') + G^>(t, \bar{t})\Sigma^A(\bar{t}, t')] + \frac{1}{i} \int_0^\beta d\bar{\tau} G^{\lceil}(t, -i\bar{\tau})\Sigma^{\lceil}(-i\bar{\tau}, t') \quad (13) \\ I^{\lceil}(t, i\tau) &= \int_0^t d\bar{t} \Sigma^R(t, \bar{t})G^{\lceil}(\bar{t}, i\tau) + \int_0^\beta d\bar{\tau} \Sigma^{\lceil}(t, -i\bar{\tau})G^M(\bar{\tau} - \tau) \quad (14) \end{aligned}$$

and  $I^{\lceil}(-i\tau, t) = [I^{\lceil}(t, -i(\beta - \tau))]^\dagger$ . The last terms in each of the Eqs. (12–14) account for the initial correlations of the systems. Time-stepping is simplified by writing the Green's function on the form  $G^{\lessgtr}(t, t') = U(t)g^{\lessgtr}(t, t')U^\dagger(t')$  where the matrix  $U(t)$  satisfies  $i\partial_t U(t) = h_{\text{HF}}(t)U(t)$ , and we have defined<sup>1</sup>  $h_{\text{HF}}(t) = h(t) + \Sigma_{\text{HF}}(t)$ . Consequently,  $g^>(T + \Delta, t') = g^>(T, t') - iU^\dagger(T) \int_0^\Delta \bar{t} U^\dagger(\bar{t}) I^>(\bar{t} + T, t')$ . Assuming  $h_{\text{HF}}$  to be constant,  $\bar{h}_{\text{HF}}$  and  $I_1^>(t, t') \approx \bar{I}_1^>(t')$  in this time-interval, we find

$$G^>(T + \Delta, t') = e^{-i\bar{h}_{\text{HF}}\Delta} G^>(T, t') - \frac{1}{\bar{h}_{\text{HF}}} [1 - e^{-i\bar{h}_{\text{HF}}\Delta}] \bar{I}_1^>(t'), \quad (15)$$

and similar expressions for  $G^<$ ,  $G^{\lceil}$ . Only the expression for  $G^<(T + \Delta, T + \Delta)$  becomes somewhat more complicated.

We have been able to propagate the Green function for a number of closed-shell atoms and diatomic molecules. The time-propagation has so far been implemented for the second-order self-energy (Fig. 2a), while the  $GW$  approximation is currently implemented only for the ground-state calculations. We can include a time-dependent electric field in the direction of the molecular axis, so that the system preserves a cylindrical symmetry. Generalizing these scheme to systems of lower symmetry does not lead to other complications than increasing the size of the calculations.

## 5. Applications

One of the many interesting quantities that can be calculated from the Green's function is the spectral function  $A(T, \omega)$ , defined according to

$$A(T, \omega) = i \int dt e^{i\omega t} [G^>(T + t/2, T - t/2) - G^<(T + t/2, T - t/2)]. \quad (16)$$

<sup>1</sup> We have here extracted the HF self-energy from the collision terms  $I$ .

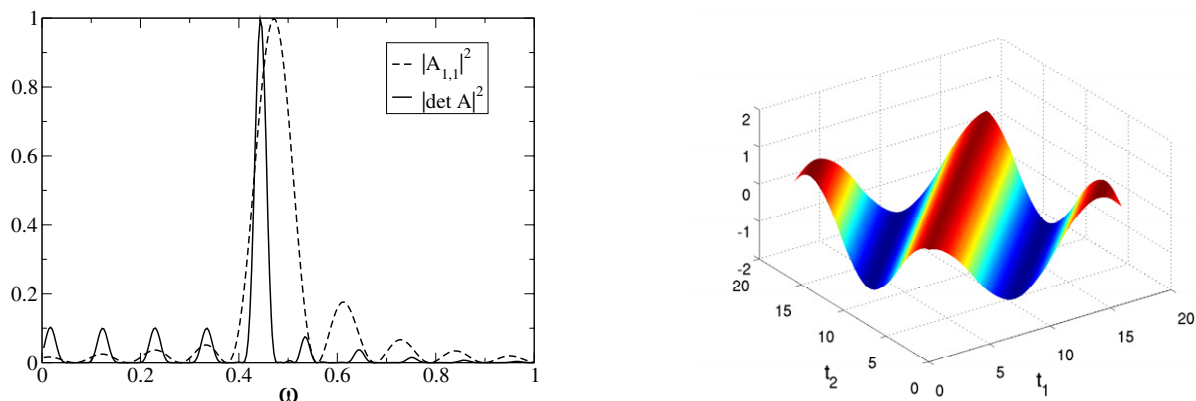


**Figure 4.** The left figure shows the spectral function of an  $\text{H}_2$  molecule in its ground state. The full line shows the determinant of the matrix  $A(\omega)$ , while the dashed line shows the matrix-element  $A_{1\sigma_g,1\sigma_g}(\omega)$ . The amplitudes have been scaled to facilitate the comparison. The figure on the right shows  $\text{Im}G_{1\sigma_g,1\sigma_g}^<(t, t')$ .

We have here introduced the time-coordinates  $T = (t_1 + t_2)/2$  and  $t = t_1 - t_2$ . If we do not add a time-dependent potential to the ground-state Hamiltonian after  $t = 0$ , the Green's function will only depend on the relative time  $t$ , and the spectral function  $A(T, \omega)$  will thus be independent of  $T$ . This is illustrated in Fig. 4. The figure shows the imaginary part of the Green's function matrix element  $G_{1\sigma_g,1\sigma_g}^<(t_1, t_2)$ , where the index  $1\sigma_g$  refers to the occupied HF orbital of the molecule. Along the  $t_1 = t_2$  diagonal, this matrix element is purely imaginary, and the amplitude is practically equal to the natural orbital occupation number. The frequency of the oscillation in the  $t_1 - t_2$  direction corresponds to the peak in the spectral function matrix element  $A_{1\sigma_g,1\sigma_g}$  as plotted in Fig. 4. The figure also shows the absolute square of the determinant of the matrix  $A(\omega)$ , which has a sharp peak at a frequency which agrees closely with the eigenvalue  $\lambda_1 = I_p + \mu$  calculated from the EKT. The plotted spectral function gives the correct position of this peak, but has additional, unphysical structure due to the fact that the Fourier transform in Eq. (16) is calculated over a finite time-interval.

The same set of functions are plotted in Fig. 5, but the Green's function is now calculated with an additional electric field switched on at  $t = 0$ . For  $t > 0$ , the field is constant, directed along the molecular axis, and has an amplitude of  $E_0 = 0.1$  a.u.. The Green's function has oscillations also along the time-diagonal, reflecting oscillations in the occupation number. The spectral function  $A(T, \omega)$  shown in Fig. 5 is calculated at  $T = 15.2$ . While the shape of the spectral function is similar to that of the ground state system, the peaks are shifted due to the applied electric field. The smaller peaks in Figs. 4 and 5 do not have any physical significance.

Time-propagation is also useful as a direct method for calculating linear response and excitation energies [17]. The excitation energies of the system can be obtained from the poles of the density response function  $\chi(\omega)$ , defined by  $\delta n(\omega) = \chi(\omega)\delta v(\omega)$ . Perturbing the system with a “kick” of the form

$$H'(t) = V\delta(t) = V \int \frac{d\omega}{2\pi}, \quad (17)$$

therefore excites all states compatible with the symmetry of the perturbing potential  $V$ . After propagating the Green's function for some time, the imaginary part of the Fourier transformed dipole moment  $d(t)$  features peaks at the frequencies corresponding to the excitation energies of the system. Time-propagation is in this way an interesting, and far more direct alternative to solving the Bethe-Salpeter equation. In Fig. 6, we have plotted the polarizability, defined



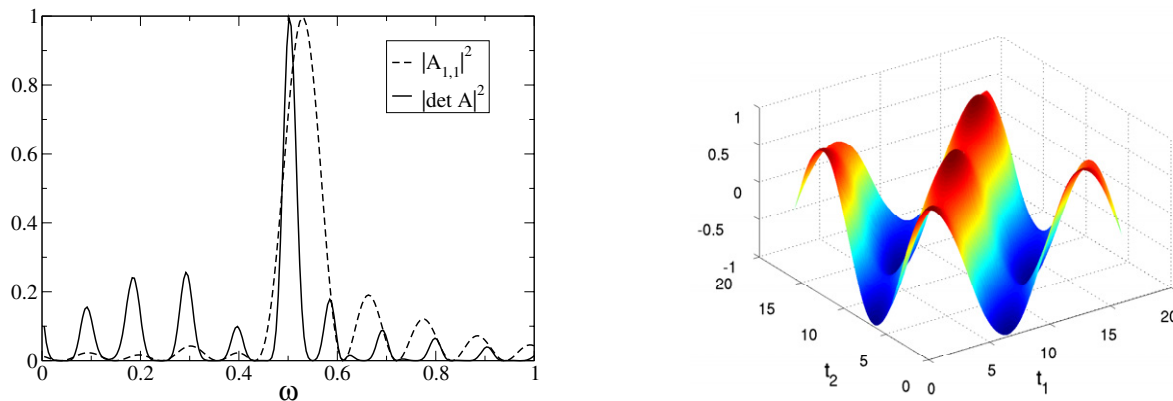


**Figure 5.** The left figure shows the spectral function  $A(T, \omega)$ , at  $T = 15.2$ , of an  $\text{H}_2$  molecule in an electric field,  $E(t) = \theta(t)E_0$ . The figure on the right shows the imaginary part of the matrix element  $\text{Im}G_{1\sigma_g, 1\sigma_g}^<(t, t')$ .

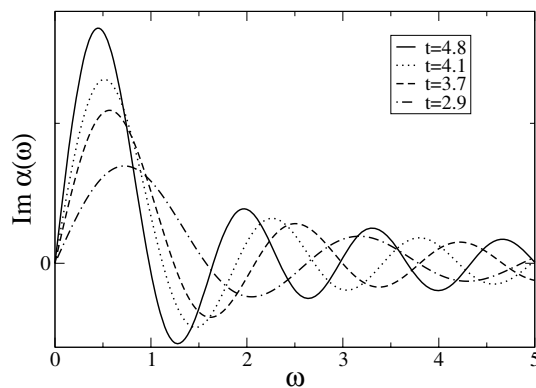


**Figure 6.** The imaginary part of the polarizability  $\alpha(\omega)$  of a beryllium atom calculated from the Green's function propagated up to a time  $t$ .

according to  $\alpha(\omega) = -1/E_0 \int dt e^{i\omega t} d(t)$ , of a beryllium atom for various durations of the time-propagation. The polarizability develops a main peak at  $\omega = 0.4$  a.u. (compared to the experimental value of 0.39), which becomes increasingly sharper as the propagation time is extended. As the system consists only of discrete energy levels, there is no significant damping in the time-dependent dipole moment  $d(t)$  as a function of time. Since the Fourier transform is taken only over a finite time-interval (i.e. the duration of the propagation), the imaginary part of the polarizability  $\alpha(\omega)$  will not always be positive, as is evident in Fig. 6. One can, somewhat artificially, remedy this by introducing an artificial damping, which will not shift the position of the excitation peak.

## 6. Future development

We are now able to propagate the Kadanoff-Baym equations for atoms and diatomic molecules. For these small systems, the second Born approximation is clearly a well-suited approximation, and the non-equilibrium Green's function is easily computed when expressed in a finite basis set. For these small systems, one can aim at quantitative agreement with experimental results, but this depends on whether the basis set is small enough for the calculations to be feasible, but

large enough to describe the details of the electron dynamics. Including molecular orbitals with large eigenenergies is important in order to account for the continuous part of the spectrum, but the rapidly oscillating terms introduced by these orbitals cause the time-propagation to be considerably less stable. The problems become more serious the larger the nuclear charge of the atoms becomes, and we are currently investigating how large systems we can do quantitatively accurate calculations for. An important goal for these calculations is to provide benchmark results for testing exchange-correlation functionals in time-dependent density functional theory. For extended systems, such as molecular chains, it becomes essential to cut down the long range of the Coulomb interaction. This is done effectively within the *GW* approximation, which we have currently implemented for the ground state. Time-propagation within the *GW* approximation does not appear to be significantly more complicated than for the second-order self-energy.

## References

- [1] Linderberg J and Öhrn Y 1973 *Propagators in Quantum Chemistry* (Academic Press:London)
- [2] Cederbaum L S and Domcke W 1977 *Adv. Chem. Phys.* **36** 205
- [3] Baym G and Kadanoff L P 1961 *Phys. Rev.* **124** 287
- [4] Baym G 1962 *Phys. Rev.* **127** 1391
- [5] Keldysh L V 1964 *Zh. Eksp. Teor. Fiz.* **47** 151 [*Sov. Phys. JETP*, **20**, 1018 (1965)]
- [6] Kadanoff L P and Baym G 1962 *Quantum Statistical Mechanics* (W. A. Benjamin, Inc.:New York)
- [7] Runge E and Gross E K U 1984 *Phys. Rev. Lett.* **52** 997
- [8] van Leeuwen R 1996 *Phys. Rev. Lett.* **76** 3610
- [9] Ku W and Eguiluz A G 2002 *Phys. Rev. Lett.* **89** 126401
- [10] Dahlen N E and van Leeuwen R 2005 *J. Chem. Phys.* **122** 164102
- [11] Luttinger J M and Ward J C 1960 *Phys. Rev.* **118** 1417
- [12] Dahlen N E and von Barth U 2004 *Phys. Rev. B* **69** 195102
- [13] Smith D W and Day O W 1975 *J. Chem. Phys.* **62** 113
- [14] Katriel J and Davidson E R 1980 *Proc Natl Acad Sci, USA*, **77** 4403
- [15] Köhler H S, Kwong N H, and Yousif H A 1999 *Comp. Phys. Comm.* **123** 123
- [16] Semkat D, Kremp D, and Bonitz M 1999 *Phys. Rev. E* **59** 1557
- [17] Kwong N-H and Bonitz M 2000 *Phys. Rev. Lett.* **84** 1768